

ording to which the Weiss limit might well play an important role only in the determination of the equilibrium properties of spin systems, and not in their dynamical behavior.

We thank Dr. H. Y. Lau *et al.* for sending us their work prior to publication.

<sup>1</sup>R. Nathans, F. Menzinger, and S. Pickart, *J. Appl. Phys.* **39**, 1237 (1968).

<sup>2</sup>M. Collins, V. Minkiewicz, R. Nathans, L. Passell, and G. Shirane, *Phys. Rev.* **179**, 417 (1969).

<sup>3</sup>V. Minkiewicz, M. Collins, R. Nathans, and G. Shirane, *Phys. Rev.* **182**, 624 (1969).

<sup>4</sup>H. Lau, L. Corliss, A. Delapalme, J. Hastings, R. Nathans, and A. Tucciarone, *Phys. Rev. Letters* **23**, 1225 (1969).

<sup>5</sup>B. Halperin and P. Hohenberg, *Phys. Rev. Letters* **19**, 700 (1967).

<sup>6</sup>B. Halperin and P. Hohenberg, *Phys. Rev.* **177**, 952 (1969).

<sup>7</sup>See the report by L. Kadanoff, *Progr. Theoret. Phys. (Kyoto)*, Suppl. **26**, 122 (1969), and references quoted there.

<sup>8</sup>K. Kawasaki, *Progr. Theoret. Phys. (Kyoto)* **39**, 1133 (1968); **40**, 11, 706, 930 (1968).

<sup>9</sup>H. Mori and H. Okamoto, *Progr. Theoret. Phys.*

(Kyoto) **40**, 1287 (1968).

<sup>10</sup>P. Résibois and M. De Leener, *Phys. Letters* **25A**, 65 (1967), and *Phys. Rev.* **178**, 806 (1969).

<sup>11</sup>M. De Leener and P. Résibois, *Phys. Rev.* **178**, 819 (1969).

<sup>12</sup>K. Kawasaki, *J. Phys. Chem. Solids* **28**, 1277 (1967).

<sup>13</sup>K. Kawasaki, *Progr. Theoret. Phys. (Kyoto)* **39**, 285 (1968).

<sup>14</sup>From the sum rule  $\int_0^\infty \Gamma_q(\omega) d\omega = \pi/2$  for the spectral function  $\Gamma_q(\omega)$ , we expect of course that  $\Gamma_q(0) = \int_0^\infty \tilde{\Gamma}_q(t) \times dt$  gives an estimate of the linewidth, although, strictly speaking, this latter is of course shape dependent.

<sup>15</sup>After this note was submitted for publication, D. Huber and D. Krieger reported a similar calculation in *Phys. Rev. Letters* **24**, 111 (1970), where a plot is given of  $\omega_\kappa(q)/\omega_\kappa(0)$  against  $(q/\kappa)^2$ . Their method is however developed mainly for  $q/\kappa \ll 1$  (because of a cutoff at  $k_m \lesssim 5\kappa$ ). Moreover, for comparison with the experiments of Lau *et al.*, they need the experimental value of  $\omega_\kappa(0)$  which is possibly subject to important resolution effects. Our solution, given in Fig. 1 (and obtained with no cutoff) is probably best in the nonhydrodynamical region  $q/\kappa \gg 1$ , where most experimental results were reported (see Fig. 1) and exhibits the observable nontrivial minimum at  $q/\kappa \approx 0.5$  which cannot be seen in the above-mentioned work; otherwise the two results agree semiquantitatively. We thank P. C. Hohenberg for pointing out this work to us.

## COVALENT BONDING AND THE NEUTRON MAGNETIC FORM FACTOR OF THE $Mn^{2+}$ ION\*

A. J. Freeman

Physics Department, Northwestern University, Evanston, Illinois 60201,  
and Argonne National Laboratory, Argonne, Illinois 60439

and

D. E. Ellis

Physics Department, Northwestern University, Evanston, Illinois 60201

(Received 23 December 1969)

Fully variational unrestricted Hartree-Fock calculations for the  $(MnF_6)^{4-}$  cluster are reported. Charge and spin densities are analyzed and shown to result in a neutron magnetic form factor which is contracted relative to the free-ion value in agreement with experiment but contrary to predictions of simple covalent-bonding theory.

Covalency or electron-transfer effects have been identified by NMR and neutron magnetic scattering experiments as playing an important, indeed vital, role in understanding the observed magnetic and optical properties of transition-metal compounds. An unresolved question is the apparent failure of covalent theory to explain the measured neutron magnetic scattering from  $Mn^{2+}$  ions in magnetic salts. These experiments show relatively little loss of intensity at low scattering angles<sup>1</sup> and a form factor which lies well below the free  $Mn^{2+}$  ion value [or an expanded spin density relative to the free-ion Hartree-Fock (H-F)

result]. By contrast,  $Ni^{2+}$  shows a large reduction in absolute intensity in the forward direction and a neutron magnetic form factor which lies above the free-ion value<sup>2</sup> (or a contracted spin density). Hubbard and Marshall<sup>3</sup> have shown, using a simple linear combination of atomic orbitals (LCAO) model, that bonding effects will raise the form factor above the free-ion value and result in a loss of intensity at low scattering angles, consistent with the  $Ni^{2+}$  results. Since core polarization<sup>4</sup> and unquenched orbital angular momentum<sup>5</sup> contributions also raise the measured form factor, the observation that the spin density in

manganese salts is expanded relative to the free ion, while the nickel density is contracted, has found no satisfactory explanation.

Various attempts have been made in recent years to understand the effects of covalent bonding on the observed properties of transition-metal ions in crystals.<sup>6</sup> Since NMR, neutron scattering, and optical experiments revealed the importance of the role played by the magnetically "inert" anions (or ligand ions), theoretical emphasis has concentrated heavily on attempts at understanding the behavior and properties of a cluster of atoms as being representative of the crystal. However, even for a cluster consisting of a single metal ion and its nearest-neighbor ligands, the computational difficulties have been formidable; the resulting calculations have suffered from approximations in the Hamiltonian and in matrix elements, insufficient variational freedom, lack of self-consistency, etc. For some time now we have been developing the unrestricted Hartree-Fock molecular-orbital self-consistent-field (UHF-MO-SCF) method<sup>7</sup> for clusters as a step in overcoming these difficulties. Here we report some results of fully variational UHF calculations for the  $(\text{MnF}_6)^{4-}$  cluster, as in  $\text{KMnF}_3$ . Expanded spin densities and contracted neutron magnetic scattering factors are obtained for the cluster relative to the free ion. These results show that covalent-bonding theory can resolve the apparent paradox between such disparate cases as  $\text{Mn}^{2+}$  and  $\text{Ni}^{2+}$ . While the open  $e_g$  shell in  $(\text{MnF}_6)^{4-}$  has a considerable admixture of ligand density, as is the case in  $(\text{NiF}_6)^{4-}$ , the open  $t_{2g}$ -shell orbitals (which point between the ligands) have expanded slightly in order to share more fully in the covalent bonding between the ligand  $p\pi$  orbitals.

Covalency has unfortunately come to be associated with the single variational parameter included into simple linear combinations of atomic orbitals—the LCAO approximation. In this "traditional" approach a minimal basis set is chosen, corresponding to occupied orbitals of the isolated ions. As a result, the coefficients  $C$ , coupling metal and ligand basis functions,

$$\Psi_i^{\text{MO}} = \sum_j \varphi_j^{\text{metal}} C_{ji} + \sum_k \chi_k^{\text{ligand}} C_{ki}, \quad (1)$$

are largely determined by orthogonality constraints, and the only free (variational) parameters are those coupling unpaired metal  $3d$  electrons to the ligands. Thus for  $(\text{NiF}_6)^{4-}$  in its  ${}^3A_{2g}$ ,  $t^6e^2$  ground state one has only to determine the coupling between metal and ligand  $e_g$  elec-

trons. For  $(\text{MnF}_6)^{4-}$  in its  ${}^6A_{1g}$ ,  $t^3e^2$  ground state one has to find both  $e_g$  and  $t_{2g}$  parameters. Even this simple program has proved difficult to carry out, and attempts to simplify the problem further (i.e., by fitting a single covalency parameter to the hyperfine data<sup>8</sup>) lead to results in conflict with the neutron measurements. In addition, a minimal LCAO basis is questionable as giving perhaps a misleading picture of the overlap and covalent mixing between ligand and metal orbitals. One would wish to allow for significant charge transfer onto the metal, expansion or contraction of  $d$  orbitals, the formation of  $s-p$  hybrid orbitals on the ligands, and the effects of spin polarization back on the open-shell electrons. All of these effects require detailed study and calculation.

Previously,<sup>6</sup> we attacked these problems for the case of  $(\text{NiF}_6)^{4-}$  by using a one-center basis set which had sufficient variational freedom to describe all these effects, and whose matrix elements were calculated to high accuracy. Even with a basis which was far from complete some of the simplicity of the LCAO picture was lost. (In fact, with any flexible basis it is impossible to give a rigorous definition of "covalency," since any partitioning into well-defined atomic sets is arbitrary.) The calculated spin density and neutron form factors were found to deviate from the free-ion  $\text{Ni}^{2+}$  values in agreement with Hubbard and Marshall's single LCAO result and in qualitative agreement with experiment. Their simple picture was essentially verified: The strong interaction of the unpaired metal  $e_g$  electrons with the ligands leads to a net charge transfer inward and a spin transfer to the ligands which results in a "peaking" of the form factor at low angles and an apparent raising of the form factor elsewhere due to the loss of intensity at low scattering angles. Of course, quantitative results were seen to depend strongly on the cumulative effects of rearrangement and bonding in all the other electron shells.

Limitations in the one-center method and developments in numerical-integration procedures have led us back to the multicenter basis for doing the UHF-MO-SCF cluster studies reported here. The basic UHF formalism for this work is straightforward.<sup>6</sup> Briefly, to obtain the MO solution  $\Psi = AC$  to the H-F equations with an orthonormal basis  $\{A_i(\vec{r})\}$ , we iteratively solve the coupled matrix eigenvalue equations

$$F \dagger C \dagger = \epsilon \dagger C \dagger, \quad F \dagger C \dagger = \epsilon \dagger C \dagger, \quad (2)$$

where  $F$  is a matrix with elements  $F_{ij}$  of the Fock operator in the given basis,  $C$  is the matrix of variational parameters defining the MO's  $\{\Psi_{ij}\}$ , and  $\epsilon$  is the (diagonal) matrix of UHF one-electron energies. The arrows  $\uparrow$ ,  $\downarrow$  label either spin.

It is well known that the most difficult aspect of solving the H-F equations for polyatomic systems has always been the evaluation of the resulting numerous multicenter integrals. We have developed a form of Monte Carlo, or more properly "open Diophantine" integration due to Haselgrove,<sup>9</sup> in which matrix elements of the Fock operator are found by numerical integration in six-dimensional space. The method converges with reasonable speed and is superior to any other method we know of for larger systems since matrix elements of the Fock operator are evaluated directly without the intermediate step of molecular integrals. Our basis sets are multicenter Slater (exponential) functions, but the method can be easily adapted to any analytic or numerical basis. Simply put, the matrix elements are evaluated numerically by a sampling procedure

$$F_{ij} = \sum W(\vec{r}_n) A_i^*(\vec{r}_n) h(\vec{r}_n) A_j(\vec{r}_n), \quad (3)$$

where  $W(\vec{r})$  is an integration weighting function,  $\{A_j(\vec{r})\}$  are the basis functions here chosen as orthogonalized linear combinations of functions  $\chi^l y^m z^n r^p e^{-\alpha r}$  centered on each nucleus, and  $h(\vec{r})$  is the H-F effective Hamiltonian.

All 83 occupied MO levels which make up the  $(\text{MnF}_6)^{4-} {}^6A_{1g}$  state were included. Basis sets for these calculations were chosen by inspecting Clementi's results for the free ions.<sup>10</sup> The 79 atomic functions  $A_j(\vec{r})$  used fall short of a complete basis but allow considerable flexibility in determining the occupied MO's. The ground state was iterated for thirty SCF cycles with 16 000 integration points in order to stabilize the electron density to four decimal places.

For our single-determinant wave function the spin density is given by

$$\rho^s(\vec{r}) = \sum_i [n_i^\uparrow |\Psi_i^\uparrow(\vec{r})|^2 - n_i^\downarrow |\Psi_i^\downarrow(\vec{r})|^2], \quad (4)$$

where  $\{n_i\}$  are the (predetermined) occupation numbers, and  $\{\Psi_{ij}\}$  are the MO solutions to (2). The scattering amplitude is defined simply as the Fourier transform of the spin density,

$$f(\vec{K}) = \int d^3r e^{i\vec{K}\cdot\vec{r}} \rho^s(\vec{r}), \quad (5)$$

where  $\vec{K}$  is the scattering vector with  $|\vec{K}| = 4\pi \times \sin\theta/\lambda$ . Here we limit ourselves to discussing

the spherical average of (5),

$$f_0(K) = \int d^3r j_0(Kr) \rho^s(\vec{r}), \quad (6)$$

where  $j_0$  is the zeroth-order spherical Bessel function. (Nonspherical terms contribute to aspherical "bumps" in the measured form factor even though the ground state is nominally spherically symmetric.<sup>4</sup>) The scattering factors are calculated by the same numerical-integration procedure used in evaluating the Fock matrix elements, i.e.,

$$f_0(K) = \sum_n \omega(\vec{r}_n) j_0(Kr_n) \rho^s(\vec{r}_n). \quad (7)$$

The results show that although the spin-polarized "closed shells" make a sizable contribution to the fluorine hyperfine parameters, their influence on the spherical scattering factor is small,  $\sim 1-2\%$  of the total. Hence we focus on the individual spin densities of the open  $e_g$  and  $t_{2g}$  shells, whose five unpaired electrons dominate the scattering. The separate contributions of the  $e_g$  and  $t_{2g}$  open shells to the scattering factor are given in Fig. 1 and reveal the qualitative differences between the two sets of orbitals. At large scattering angle, the  $e_g$  form factor closely follows that of the free ion; at smaller angles ( $\sin\theta/\lambda \sim 0.25$ ), the strong admixture of fluorine spin density pulls its form factor below

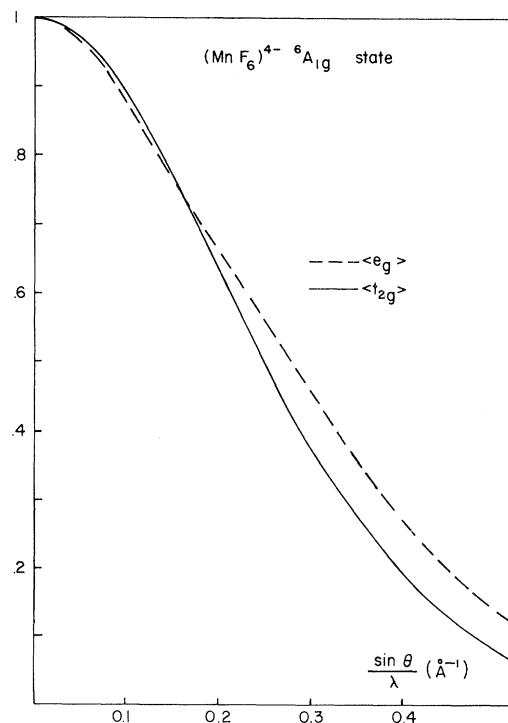


FIG. 1. The spherical scattering factors for  $e_g$  and  $t_{2g}$  densities.

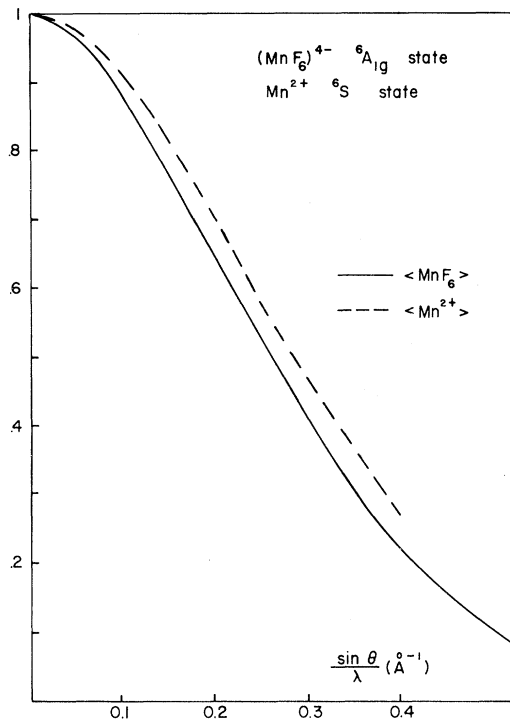


FIG. 2. Comparison of  $f_0$  scattering factors for  $(\text{MnF}_6)^{4-} \text{}^6A_{1g}$  and free-ion  $\text{Mn}^{2+} \text{}^6S$  states.

the free-ion result—giving a shoulder similar to that found in  $\text{NiF}_6$  (which has only the open  $e_g$  shell). The  $t_{2g}$  scattering, however, lies everywhere below the free-ion scattering and is best described by an overall expansion of the metal  $d$  orbital rather than an admixture of fluorine density.

In Fig. 2 we compare the spherical scattering factor  $f_0$ , calculated for the unpaired  $t_{2g}$  and  $e_g$  electrons but normalized to unity, for the free  $\text{Mn}^{2+}$  ion in the  $\text{}^6S$  state and for the  $(\text{MnF}_6)^{4-}$  cluster in the  $\text{}^6A_{1g}$  state. The  $\text{Mn}^{2+}$  scattering factor was calculated from a wave function obtained with the same atomic basis set as used in the cluster, to avoid any possible bias in comparing the free-ion and cluster results. (The atomic basis set for  $\text{Mn}^{2+}$  was substantially reduced from that of accurate analytic H-F calculations,<sup>11</sup> i.e., only two Slater AO's were used to represent the  $3d$  orbitals. The effect of this basis is to give a free-ion form factor which is expanded relative to the H-F form factor for  $\text{Mn}^{2+}$ ; hence, no absolute accuracy can be attached to the individual results. Comparison between the two calculations is physically meaningful.) The results show that the  $\text{MnF}_6$  form factor is everywhere reduced compared with the free-ion value and substantially in accord with the neu-

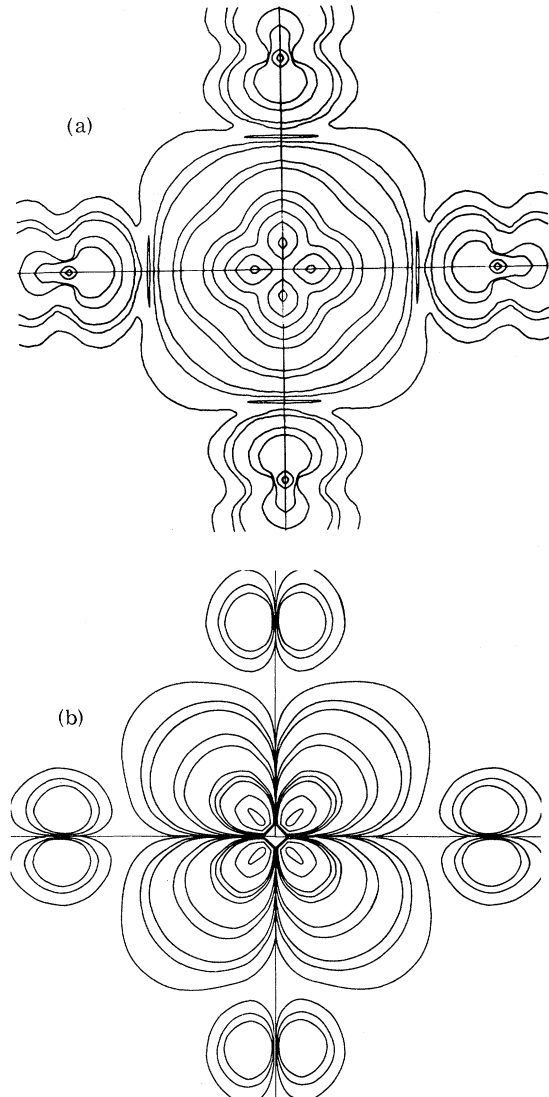


FIG. 3. Spin-density contours in the  $z=0$  plane for (a)  $e_g$  and (b)  $t_{2g}$  representations. Contour levels are shown at 1.0, 0.5, 0.25, 0.10, 0.05, 0.01, 0.005, 0.001, 0.0005, and 0.0001 in  $a_0^{-3}$  units.

tron data. (As stated, scattering due to the core polarization has been calculated to be only 1-2% of the total and is not included in Fig. 2.)

In order to understand the physical origin of the contracted form factor observed for  $\text{Mn}^{2+}$  and apparently reproduced by our calculations, we have prepared contour maps of the charge and spin densities for the individual  $t_{2g}$  and  $e_g$  symmetries. Examination of the  $e_g$  charge density shows strong admixture of metal "3d" and ligand  $2s$  and  $2p\sigma$  orbitals as was seen earlier for the case of  $\text{Ni}^{2+}$ . However, the  $t_{2g}$  charge density shows that the "3d" density is expanded in the (111) directions relative to the free-ion

values. This expansion apparently occurs in order for the  $t_{2g}$  orbital to form a covalent "bridge" between the  $p\pi$  orbitals on the different  $F^-$  centers. While a small expansion was found in earlier point-charge crystal-field calculations,<sup>4</sup> such a covalent bridge further serves to minimize the energy of the system in much the same (well-known) way that the covalent bonding bridge is established between the metal  $3d$  and ligand  $2s$  and  $2p\sigma$  in the  $e_g$ -symmetry case. Some of these effects are shown in Fig. 3 where  $e_g$  and  $t_{2g}$  spin-density contours are plotted in the  $z=0$  plane. The large induced spin density at the fluorine site is evident for the  $e_g$  case. The  $t_{2g}$  contour map shows the weaker  $p\pi$  spin-density arrangement about the fluorine sites and the expanded spin density into the region between the ligands.

\*Work supported by the Air Force Office of Scientific Research, the U.S. Atomic Energy Commission, and

the Advanced Research Projects Agency through the Northwestern University Materials Science Center.

<sup>1</sup>J. M. Hastings, N. Elliot, and L. M. Corliss, *Phys. Rev.* **115**, 13 (1959); R. Nathans, H. A. Alperin, S. J. Pickart, and P. J. Brown, *J. Appl. Phys.* **34**, 1182 (1963), and references therein.

<sup>2</sup>H. A. Alperin, *Phys. Rev. Letters* **6**, 55 (1961).

<sup>3</sup>J. Hubbard and W. Marshall, *Proc. Phys. Soc. (London)* **86**, 561 (1965).

<sup>4</sup>R. E. Watson and A. J. Freeman, *Phys. Rev.* **120**, 1125, 1134 (1960).

<sup>5</sup>M. Blume, *Phys. Rev.* **124**, 96 (1961).

<sup>6</sup>D. E. Ellis, A. J. Freeman, and P. Ros, *Phys. Rev.* **176**, 688 (1968), and references therein.

<sup>7</sup>D. E. Ellis and A. J. Freeman, *J. Appl. Phys.* **39**, 424 (1968), and *Bull. Am. Phys. Soc.* **13**, 482 (1968).

<sup>8</sup>R. G. Shulman and K. Knox, *Phys. Rev. Letters* **4**, 603 (1960); B. E. F. Fender, A. J. Jacobson, and F. A. Wedgwood, *J. Chem. Phys.* **48**, 990 (1968).

<sup>9</sup>C. B. Haselgrove, *Math. Computation* **15**, 323 (1961); H. Conroy, *J. Chem. Phys.* **47**, 5307 (1967); D. E. Ellis, *Intern. J. Quant. Chem.* **2S**, 35 (1968).

<sup>10</sup>E. Clementi, *IBM J. Res. Develop. Suppl.* **9**, 2 (1965).

<sup>11</sup>R. E. Watson, *Phys. Rev.* **118**, 1036 (1960).

## ELECTRICAL RESISTIVITY OF NICKEL NEAR THE CURIE POINT\*

F. C. Zumsteg and R. D. Parks

Department of Physics and Astronomy, University of Rochester, Rochester, New York 14627

(Received 22 December 1969)

Emphasis is placed on the temperature dependence of the magnetic resistance  $R_{\text{mag}}$  in the region  $10^{-4} \lesssim |\epsilon| \lesssim 10^{-2}$ , where  $\epsilon = (T - T_c)/T_c$ . The temperature dependence of  $dR_{\text{mag}}/dT$  is found to be the same, within experimental error, as that of the specific heat, both above and below  $T_c$ . The anomalous behavior in the region  $0 \lesssim \epsilon \lesssim 5 \times 10^{-3}$  reported by Craig, Goldberg, Kitchens, and Budnick is not observed.

Studies of transport properties offer the possibility of significantly enhancing our knowledge of microscopic processes near second-order phase transitions. The importance of such studies is well documented, together with a historical sketch of developments in the field, in the recent review article by Craig and Goldberg.<sup>1</sup> The theory of critical transport properties is virtually unexplored and appropriate experimental data are sparse. An exception to the latter deficiency is provided by existing data on the electrical resistivity of nickel. Measurements within  $|\epsilon| \sim 5 \times 10^{-3}$  of  $T_c$  have been reported by Kraftmakher<sup>2</sup> and measurements within  $|\epsilon| \sim 5 \times 10^{-4}$  of  $T_c$  have been reported by Craig and co-workers.<sup>3</sup> In both instances, a divergence in the temperature derivative of the magnetic resistivity at  $T_c$  was observed. This divergence was found to resemble (quantitatively<sup>2,3</sup> for  $\epsilon \gtrsim 5 \times 10^{-3}$  and qualitatively<sup>2</sup> for  $-\epsilon \gtrsim 5 \times 10^{-3}$ ) the divergence in the

magnetic specific heat.<sup>4,5</sup> The theoretical basis of such a correspondence has been discussed by Mannari<sup>6</sup> and by Fisher and Langer,<sup>7</sup> and will be further discussed below.

A second and perhaps more dramatic effect reported by Craig and co-workers<sup>3</sup> is a distinct change in the temperature dependence of  $dR_{\text{mag}}/dT$  at approximately  $\epsilon = 5 \times 10^{-3}$ . It was observed that this is the temperature at which the (temperature dependent) magnetic coherence length  $\xi(T)$  approximately equals the phonon-limited mean free path of the conduction electrons. Craig and Goldberg<sup>1</sup> suggested that this effect marks the transition from the hydrodynamic regime to the critical regime predicted by dynamic scaling theory. Hargitai<sup>8</sup> has suggested that the origin of the anomaly lies in a strong temperature dependence of the phonon-limited mean free path in the vicinity of  $T_c$ .

In this Letter we report new results which cor-